

## Densely integrated photonic devices based on microring resonators for use in access networks

Edwin J. Klein<sup>1</sup>, Gabriel Sengo<sup>1</sup>, Lucy T. H. Hilderink<sup>1</sup>, Marcel Hoekman<sup>1</sup>, Rudy Pellens<sup>2</sup>, Paul van Dijk<sup>2</sup>, and Alfred Driessen<sup>1</sup>

<sup>1</sup>Integrated Optical MicroSystems Group, MESA+ Research Institute, University of Twente, P.O.Box 217, 7500 AE Enschede, The Netherlands (email: [e.j.klein@utwente.nl](mailto:e.j.klein@utwente.nl))

<sup>2</sup>ASML, The Netherlands (email: [Paul.van.Dijk@asml.com](mailto:Paul.van.Dijk@asml.com))

**Abstract:** A reconfigurable optical add-drop multiplexer as well as a 1x4x4 reconfigurable  $\lambda$  router, designed for use in the second telecom window, are demonstrated. The devices that each have a footprint less than 2 mm<sup>2</sup> are based on thermally tunable vertically coupled microring resonators fabricated in Si<sub>3</sub>N<sub>4</sub>/SiO<sub>2</sub>.

**Keywords:** optical networks, optical add-drop multiplexer, optical cross-connect, integrated optics, thermally tunable, microring resonator, Si<sub>3</sub>N<sub>4</sub>

### Introduction

The application of optical fibers has led to virtually loss-less point to point data links in the core network with practically unlimited bandwidth. In response to the ever increasing bandwidth demands of consumers the optical techniques employed in these networks are now gradually extended towards the consumers premises with the ultimate goal of enabling ubiquitous high-speed network access for everyone. At the access network level, where equipment is shared by a few users at the most, cost is the major issue. In addition the demand of optical transparency at the nodes and hubs, requiring no conversion between the optical and electrical domains, results in a high degree of complexity of the devices.

In our opinion, the answer to the challenges of cost and complexity will be mass-produced very large scale integrated (VLSI) photonics [1]. Promising building blocks in these devices are Microring Resonators (MRs) [2,3] built using high refractive index waveguides which can be used to create densely integrated wavelength filters as well as more complex functionality [4-7]. The high degree of integration that can be achieved with these micro-resonators is demonstrated by the mask layout in figure 1. This mask layout, which was created from the overlay of multiple stepper reticle images, defines a wafer area of only 1 x 1 cm<sup>2</sup> yet contains five 4-channel WDM routers and several test structures. In fact, the minimum size of the components shown in this layout was not limited by the size of the micro-resonators, but rather the size of the electrodes used to tune the resonators and the 250  $\mu$ m spacing between the in- and output waveguides required for the fiber-chip coupling for these devices.

The design, fabrication and measurements of the densely integrated WDM router [5] shown in figure 1 as well as a less complex 4-channel reconfigurable Optical Add Drop Multiplexer (ROADM), both intended for use in the second telecom window, will be presented in this paper.

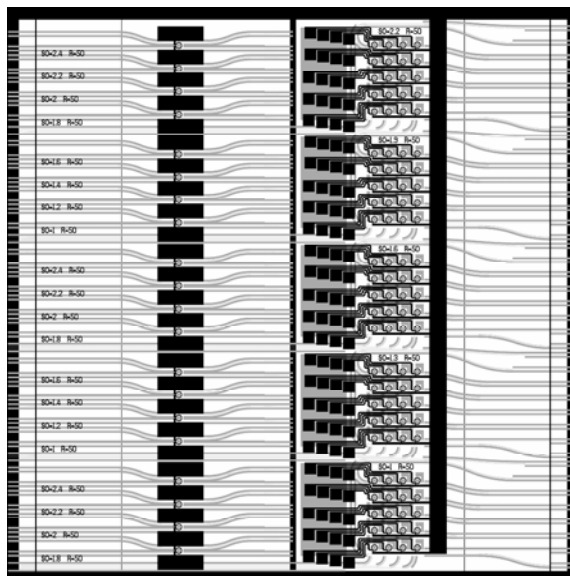


Figure 1. Mask lay-out of 5 WDM routers (right) and a number of test structures (left); the layout is equivalent to an on-wafer area of 1 x 1 cm<sup>2</sup>.

## Design and fabrication

The schematic layouts of the OADM and the router are given in figure 2. The OADM consists of a central bus waveguide along which four resonators are placed. These resonators can be used to add or drop channels to and from the eight port waveguides. The router consists of a single de-multiplexer and a routing matrix. The de-multiplexer consists of four resonators that de-multiplex up to four channels from the input port. These channels can then be combined in any combination by the routing matrix and sent to any of the four drop ports. Both devices have been designed using the same basic resonator building block. The resonator building blocks in the OADM are vertically spaced at  $250\ \mu\text{m}$ . Although a smaller spacing is possible, this is not practical since the device has been designed to interface with a fiber array with a fiber pitch of  $250\ \mu\text{m}$ . For the router the vertical spacing between the drop-port waveguides is  $300\ \mu\text{m}$  due to electrode wiring requirements. The resonator building block in both devices uses a cross-grid waveguide approach [5], in which the two waveguides that couple to the MR cross each other. All of the resonators are made thermally tunable using a thin-film omega-shaped chromium heater. A 3D geometry and cross-section of the 3D MR are shown in figure 3. The resonator has a radius of  $50\ \mu\text{m}$  and is implemented using a ridge waveguide with a total thickness of  $180\ \text{nm}$ . The port waveguides also consist of a ridge waveguide having a total thickness of  $140\ \text{nm}$ . The microring resonators have been designed to work exclusively with the TE polarization.

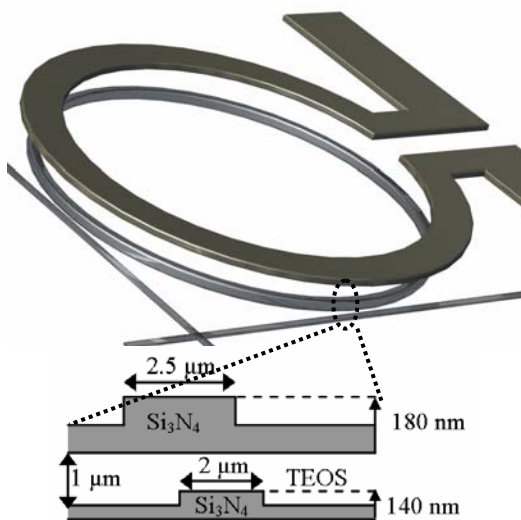


Figure 3: MR top view and coupling region cross-section.

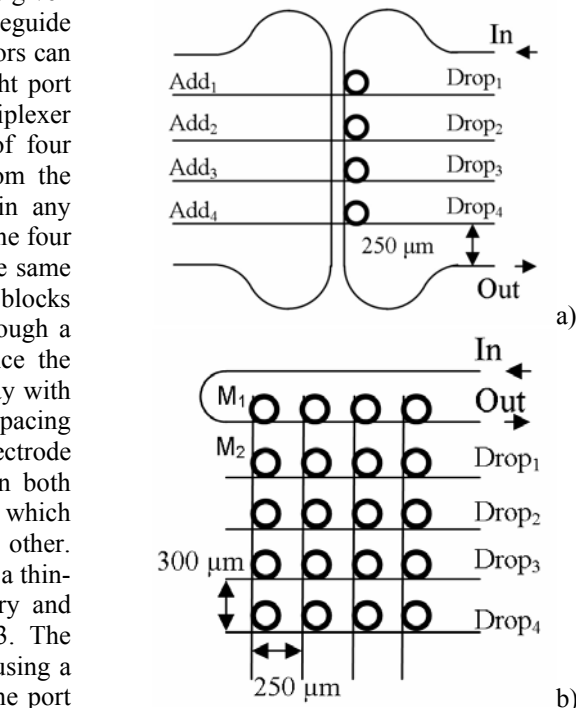


Figure 2: Schematic layout of an OADM a) and b)  $1 \times 4 \times 4\ \lambda$ -router.

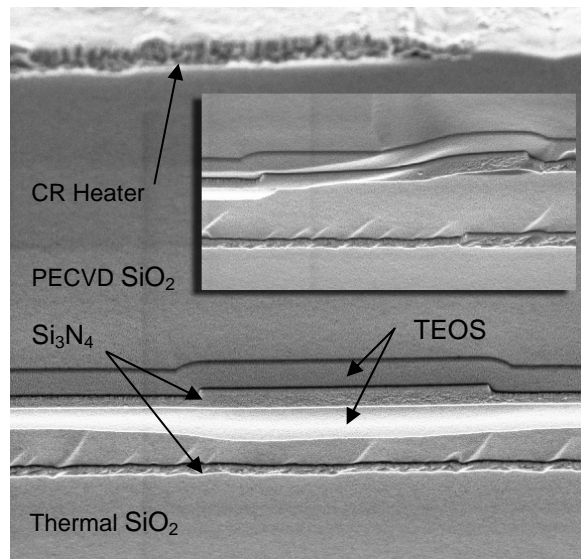


Figure 4: SEM micrograph of the cross-section of a MR. The inset shows the cross-section of a MR fabricated without using CMP. The resonator is "lifted up" due to the waveguide underneath.

A major concern in the fabrication of vertically coupled micro-resonators [8] is the correct alignment of the resonator to the port waveguides. In previously demonstrated devices [6,7], fabricated using contact lithography, the alignment was improved by using a nonius-type approach of built in deviations in the alignment. This, however, significantly lowered the yield. A combination of stepper and contact lithography was therefore used in these new devices to improve yield and increase the alignment accuracy. Contact lithography was used to define

the non-critical layers, such as the electrodes, while the critical resonator and port waveguide layers were defined using an ASML PAS-5500/275 stepper tool. With this tool these layers could be aligned with an accuracy better than 100nm. To facilitate the use of the stepper, alignment markers were first etched into a bare silicon wafer. This wafer was then thermally oxidized to a thickness of 6  $\mu\text{m}$  after which a 140 nm thick layer of LPCVD  $\text{Si}_3\text{N}_4$  was grown on top [9]. After exposure using the stepper the port waveguides were then etched in this layer using reactive ion etching (RIE). A 1  $\mu\text{m}$  TEOS separation layer was deposited next. Because the TEOS layer closely follows the topography of the underlying layers this layer was chemically mechanically polished (CMP). This is important because without it the “lifting up” of the resonator that occurs when the resonator lies on top of a port waveguide, as shown in the inset in figure 4, can significantly increase the roundtrip losses in the resonator. After the CMP the  $\text{Si}_3\text{N}_4$  resonator layer was deposited, exposed with the stepper and etched using RIE. A passivation layer consisting of 0.5  $\mu\text{m}$  TEOS and 3.5  $\mu\text{m}$  PECVD  $\text{SiO}_2$  were deposited next after which the device was annealed at 1150°C. On top of this layer stack, of which a cross-section is shown in figure 4, 200 nm thick chromium heaters and gold leads were created using contact lithography in combination with lift-off.

## Measurement results and discussion

The realized OADM, of which a picture is shown in figure 5, was measured using a broadband source and an optical spectrum analyzer with a resolution of 0.05 nm. Figure 6 shows the normalized responses measured for the four drop ports when the broadband source was connected to the “In” port of the OADM (see figure 2a). To demonstrate the dropping of four different channels to these ports the resonance frequency of each resonator in the OADM has been tuned to a different wavelength. In the drop port responses the effects of channels dropped by adjacent MRs can be observed, for instance in the response at the fourth drop port. The three dips in the response of this port are the through responses of the three preceding resonators. For the drop port responses shown the filter rejection ratio of the individual resonators is  $\approx 16.7$  dB. From the measurements the amplitude coupling constants of the

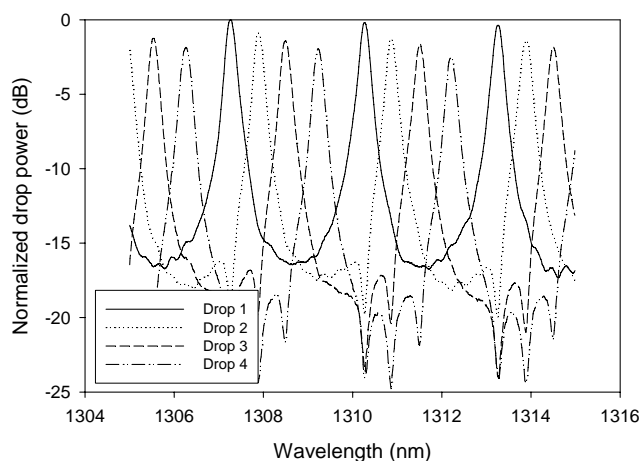


Figure 6: Drop Responses of Drop<sub>1</sub>-Drop<sub>4</sub> for a broadband source connected to the “In” port.

heaters on all resonators are switched off and all resonators are in resonance at the same wavelength. The spectral response of this configuration shows a single broad peak, with a FSR of 3 nm. This peak is predominantly the result of the power dropped by the first resonator in the de-multiplexer section of the router (M1 in figure 2b). The minor dip in the center of the peak is due to the interaction with the (smaller) power fractions dropped by subsequent resonators in the de-multiplexer. For the second configuration the first resonator was tuned half a FSR. The power dropped by this resonator shows up as the minor peak in the response. The major peak is now the result of the power dropped by the second resonator in the de-multiplexer and the interactions with the third and fourth resonators. For the third and final router configuration resonator M2 was

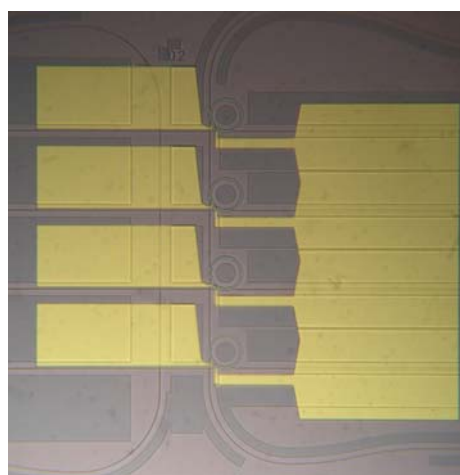


Figure 5: Realized OADM.

individual resonators were determined to be  $\kappa_1 = \kappa_2 = 0.40 \pm 0.01$  and the resonator losses  $33 \pm 3$  dB/cm. The FSR and Finesse are 3.0 nm and 10.6 respectively, giving a FWHM of 0.28 nm ( $\approx 46$  GHz @1310 nm). The channel crosstalk for channels spaced at 100 GHz (0.6 nm @1300 nm) is  $\approx -12$  dB. The considerable losses in the resonator are due to ridge height of the resonator, which was not etched deep enough. These losses also resulted in relatively high on-chip insertion losses of the resonators of  $\approx 5$  dB. The  $\lambda$ -router, shown in figure 7, has also been characterized using the broadband source at the input and the OSA to measure the wavelength response of the first drop port (see figure 2b). In figure 8 the responses measured at this port are given for three different “tuning” configurations of the router. In the first configuration the

tuned to the same wavelength as M1. This causes the channel selected by M1 to be dropped by M2 onto the first drop port. The channel is therefore effectively switched “on” on this port for this configuration as is shown by the large peak in the response measured for this configuration. A comparison with the response of the second configuration shows that the “on” / “off” switch ratio that can be obtained for this router is  $\approx 15$  dB. Also the FWHM of the dropped channel is 0.22 nm ( $\approx 37$  GHz @1310 nm), making it suitable for use in next generation access networks that require bandwidths of up to 10 GHz.

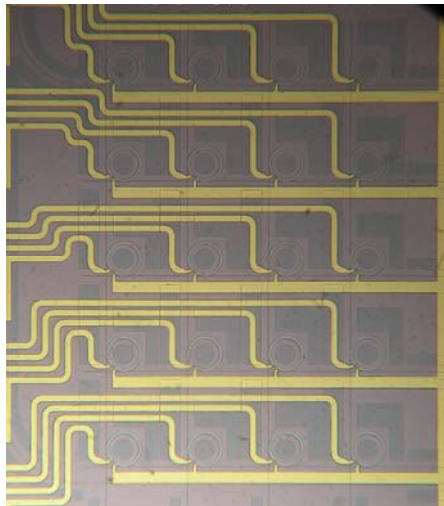


Figure 7: Realized 1x4x4  $\lambda$ -router.

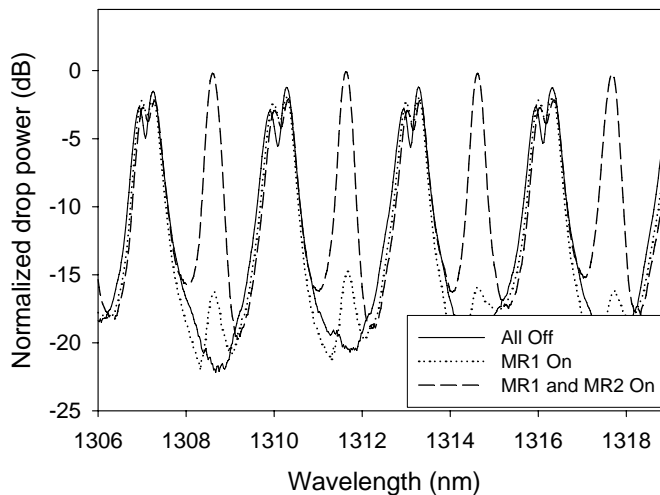


Figure 8: Switching of a single channel in the router

## Conclusions

We have presented a reconfigurable 4-channel OADM and a 1x4x4 channel  $\lambda$ -router based on  $\text{Si}_3\text{N}_4/\text{SiO}_2$ . Due to the use of microring resonators these devices are able to combine a large functionality with a small footprint: less than  $2 \text{ mm}^2$  for the devices discussed here. These devices therefore have the potential to enable more cost effective solutions for bringing fiber based networks all the way to the consumer. In addition, to our knowledge basic routing functionality of a micro-resonator based reconfigurable router has been demonstrated for the first time.

## Acknowledgements

The authors would like to thank LioniX B.V for their contributions to the fabrication of the OADM and router devices. The work has been carried out with the financial support of the Dutch Freeband Communication Project “Broadband Photonics”.

## References

- 1) B.Little et al., ‘Microring resonator arrays for VLSI photonics’, IEEE Phot. Techn. Letters, vol. 12, pp. 323-325, 2000
- 2) S.Suzuki et al., ‘Integrated –optic ring resonators with two stacked layers of silica waveguide on Si’, IEEE Phot. Techn. Letters., vol. 4(11), pp. 1256-1258, 1992
- 3) F.C. Blom et al., ‘Experimental study of integrated-optics microcavity resonators: Toward an all-optical switching device’, Appl. Phys. Letters, vol. 71, pp. 747-749, 1997
- 4) B.Little et al., ‘Microring resonator channel dropping filters’, J. of Lightw. Technology, vol. 15, pp. 998-1005, 1997
- 5) R. A. Soref et al. ‘Proposed N-Wavelength M-Fiber WDM Crossconnect Switch Using Active Microring Resonators’, IEEE Phot. Techn. Letters, vol. 10, no. 8, 1998.
- 6) E.J.Klein et al., ‘Reconfigurable add-drop multiplexer using microring resonators’, IEEE Phot. Techn. Letters, vol. 17, no. 11, pp. 2358-2360, 2005
- 7) D.H.Geuzebroek et al., ‘Compact wavelength-selective switch for gigabit filtering in access networks’, IEEE Phot. Techn. Letters, vol. 17, no. 2, pp. 336-338, 2005.
- 8) D.Klunder et al., ‘Vertically and laterally waveguide-coupled cylindrical microresonators in  $\text{Si}_3\text{N}_4$  on  $\text{SiO}_2$  technology’, Appl. Phys. B, vol. 73, pp. 603-708, 2001
- 9) K.Worhoff et al., ‘Silicon oxinitride – a versatile material for integrated optics applications’, J. Electrochemical Society, vol. 149(8), pp. F85-F91, 2002